Incremental steps toward incompatibility revealed by Arabidopsis epistatic interactions modulating salicylic acid pathway activation

Rubén Alcázar[a], Ana V. García[b], Jane E. Parker[b], and Matthieu Reymond[a,1]

[a]Department of Plant Breeding and Genetics, Max Planck Institute for Plant Breeding Research, D-50829 Köln, Germany; and [b]Department of Plant Microbe Interactions, Max Planck Institute for Plant Breeding Research, D-50829 Köln, Germany

Communicated by Maarten Koornneef, Wageningen University and Research Centre, Wageningen, The Netherlands, November 19, 2008 (received for review September 3, 2008)

Plant growth is influenced by genetic factors and environmental cues. Genotype-by-environment interactions are governed by complex genetic epistatic networks that are subject to natural selection. Here we describe a novel epistatic interaction modulating growth in response to temperature common to 2 Arabidopsis recombinant inbred line (RIL) populations (L*er* × Kas-2 and L*er* × Kond). At 14 °C, lines with specific allele combinations at interacting loci (incompatible interactions) have severe growth defects. These lines exhibit deregulated cell death programs and enhanced disease resistance. At 20 °C, growth defects are suppressed, but a positive trait of enhanced resistance is retained. Mapping of 1 interacting QTL to a cluster of *RPP1*-like *TIR-NB-LRR* genes on chromosome 3 is consistent with our finding that environmentally conditioned epistasis depends on activation of the salicylic acid (SA) stress signaling pathway. The nature of the epistatic interaction conforms to the Dobzhansky-Muller model of genetic incompatibility with incomplete penetrance for reproductive isolation. Variation in fitness of different incompatible lines reveals the presence of additional modifiers in the genetic background. We propose that certain interacting loci lead to an optimal balance between growth and resistance to pathogens by modulating SA signaling under specific environments. This could allow the accumulation of additional incompatibilities before reaching complete reproductive isolation.

natural variation | Dobzhansky-Muller interactions | growth | temperature | TIR-NB-LRR

Plants are constantly challenged by environmental fluctuations and have evolved mechanisms of tolerance and adaptation to overcome unfavorable conditions. Arabidopsis occurs in the wild over a broad range of climatic conditions and displays a high degree of phenotypic and genotypic variation (1) and a high rate of self-pollination (2). Arabidopsis is therefore a suitable model to investigate genotype-by-environment (G × E) interactions in plants. By using natural variation as a source of genetic diversity, the different polymorphisms detected between accessions have experienced "filtering" by natural selection (3). Thus, they might harbor neutral mutations or mutations that contribute positively to plant fitness in a particular environment, as deleterious mutations would produce poorly adapted individuals. The effect of a mutation on fitness can also be influenced by alleles present at other loci. These epistatic interactions represent a fundamental force in many aspects of adaptive evolution (4). The Dobzhansky-Muller (D-M) model of reproductive isolation is an example of an epistatic interaction that influences fitness traits. The model posits that hybrid sterility and inviability result from negative epistatic interactions between alleles at a minimum of 2 loci (5, 6). Separate alleles function normally in a nonhybrid genetic background and must coexist in the same genome to release deleterious effects from the epistatic interaction. Autoimmune responses leading to hybrid necrosis have been shown to condition certain D-M-type genetic incompatibilities in Arabidopsis (7).

Complex phenotypes such as growth-related traits result both from interactions between genes and with environmental factors. Even severe growth defects observed in incompatible hybrids can be attenuated by the environment (8). By taking into account the effect of G × E interactions in a genetic background, the number of potential negative epistatic interactions can increase, thereby facilitating the accumulation of incompatibilities (8). Although environmental factors have been traditionally classified as biotic or abiotic, evidence points to extensive crosstalk between these stress signaling pathways, often mediated by interactions between different phytohormone systems (9).

We examined the growth of different Arabidopsis recombinant inbred line (RIL) populations at a temperature that wild plants normally experience in nature (14 °C, also referred to as low) compared with standard laboratory conditions (20 °C, moderate). Here we describe an epistatic interaction severely influencing growth that is common to 2 RIL populations in response to low temperature. The nature of the interaction resembles that postulated by the D-M model, though it exhibits an incomplete penetrance for reproductive isolation and involves a unique epistatic network that partially overlaps with a Uk-1/Uk-3 incompatible interaction previously described in Arabidopsis (7). One of the interacting QTL maps within a cluster of *TIR-NB-LRR* (toll/interleukin-1 receptor-nucleotide binding-leucine rich repeat) *RPP1*-like genes on chromosome 3, homologs of which are known to recognize specific pathogen effectors and trigger SA-dependent defenses (10, 11). We establish that defects on growth driven by the environmentally conditioned interaction depend on activation of the SA stress signaling pathway. Epistatic interactions affect resistance thresholds in response to disease influencing growth and necrosis of hybrid plants. We show that an epistatic interaction can contribute positively or negatively to plant fitness depending on its environment by modulating the SA response. This could permit accumulation of multiple allele incompatibilities during evolution before reaching complete reproductive isolation.

Author contributions: R.A., A.V.G., J.E.P., and M.R. designed research; R.A., A.V.G., and M.R. performed research; R.A., A.V.G., J.E.P., and M.R. analyzed data; and R.A., J.E.P., and M.R. wrote the paper.

The authors declare no conflict of interest.

Data deposition: The sequence reported in this paper has been deposited in the GenBank database [accession no. FJ446580 (QTL 3 in L*er*)].

[1]To whom correspondence should be addressed at: Max Planck Institute for Plant Breeding Research, Department of Plant Breeding and Genetics, Carl-Von-Linné-Weg 10, D-50829 Köln, Germany. E-mail: reymond@mpiz-koeln.mpg.de.

This article contains supporting information online at www.pnas.org/cgi/content/full/0811734106/DCSupplemental.

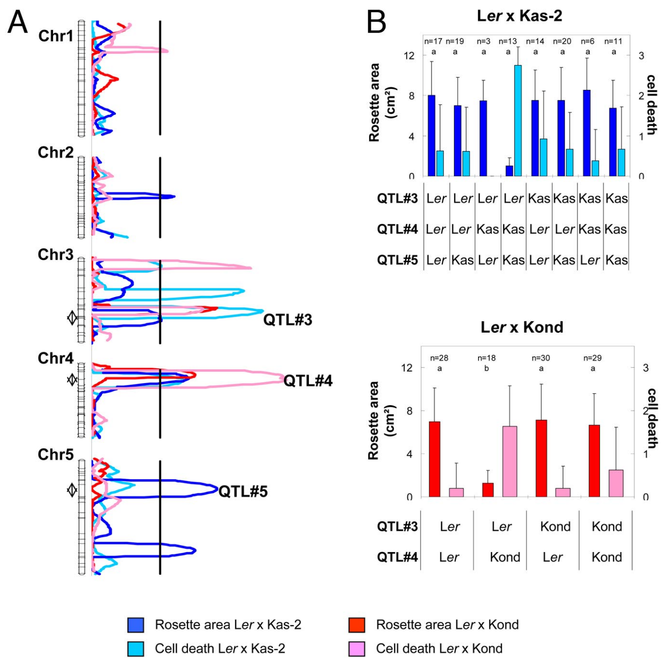

Fig. 1. Detection of QTL of rosette area and cell death at low temperature. (*A*) LOD trace for the QTL detection involved in variation of rosette area and cell death at low temperature in *Ler* × Kas-2 and *Ler* × Kond RIL. (*B*) Rosette area and cell death score of *Ler* × Kas-2 (*Top*) and *Ler* × Kond (*Bottom*) RILs sorted according to the allelic values at interacting loci QTL 3, QTL 4, and QTL 5. Values with different letters are significantly different at level $P < 0.001$ in a Student-Newman Keuls test (SNK). n, number of RIL from each class; bars, SD.

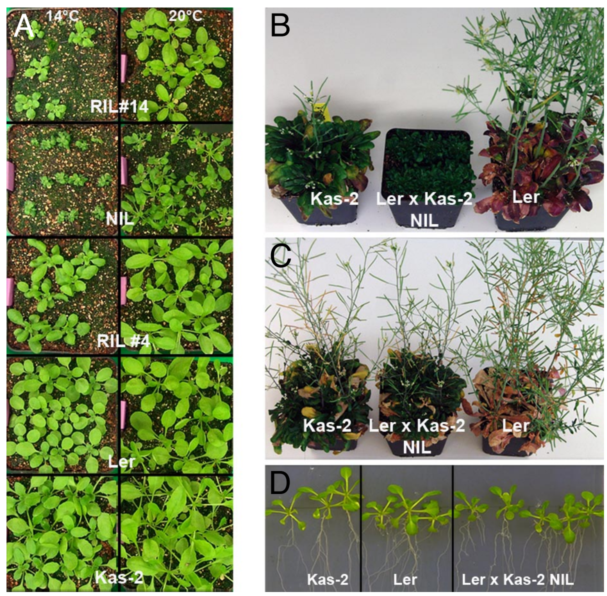

Fig. 2. Developmental phenotypes of incompatible lines. (*A*) Five-week-old *Ler* × Kas-2 incompatible lines (14, 4, and NIL) and parental accessions *Ler* and Kas-2 at 14 °C (*Left*) and 20 °C (*Right*). (*B*) Eight-week-old NIL at 14 °C and at 20 °C (*C*) compared with *Ler* and Kas-2 parents. (*D*) Two-week-old NIL grown at 14 °C under high humidity conditions.

Results

Epistatic Interactions Modulate Plant Growth in Response to Temperature. Different RILs derived from crosses between the Arabidopsis accessions Landsberg *erecta* (*Ler*) and Cvi, Sha, An-1, Eri-1, Kas-2, or Kond (12) were grown at moderate (20 °C) and low (14 °C) temperature. Reduction of rosette area in response to low temperature was most obvious among *Ler* × Kas-2 and *Ler* × Kond RILs. A subset of RILs (15% from *Ler* × Kas-2 and 24% from *Ler* × Kond; supporting information (SI) Fig. S1) were dwarf at 14 °C but resembled parental lines at 20 °C. We therefore selected these 2 populations for QTL detection and further study. Common QTL for rosette area were detected among these populations on the bottom of chromosome 3 (QTL 3) and the top of chromosome 4 (QTL 4) (Fig. 1*A*). In both populations, *Ler* alleles on QTL 3 contributed to a reduction of rosette area, whereas *Ler* alleles on QTL 4 produced the opposite effect. Because the dwarf phenotype was observed in RILs but not in the parental lines, we reasoned that the dwarfism likely results from an epistatic interaction between parental alleles. In both populations a common epistatic interaction between 2 loci was found (Fig. S2). These loci are located on QTL 3 and QTL 4. An additional epistatic interaction was revealed in *Ler* × Kas-2 involving loci located on QTL 4 and at the top of chromosome 5 (QTL 5) (Fig. 1*A* and Fig. S2). Together, the data indicate that a 3-way interaction between QTL 3, QTL 4, and QTL 5 in *Ler* × Kas-2 and a 2-way interaction between QTL 3 and QTL 4 in *Ler* × Kond condition variation of rosette area. To test this hypothesis, an ANOVA test was performed. The 3-way interaction in *Ler* × Kas-2 explained 35.5% ($P_{\mathrm{value}} < 0.001$) and the 2-way interaction in *Ler* × Kond 36.3% ($P_{\mathrm{value}} < 0.001$) of the variation in rosette area, and only a specific allele combination lead to dwarf plants (Fig. 1*B*). We concluded that the main-effect QTL are interacting. We refer to lines carrying such allele combinations as incompatible.

The allelic forms that result in dwarfism on QTL 3 and 4 behaved recessively in both populations, whereas the incompatible Kas-2 allele on QTL 5 was dominant. All crosses derived from incompatible *Ler* × Kas-2 and *Ler* × Kond RILs resulted in dwarf F_1 plants at low temperature. This phenotype and the recessive nature of QTL 4 alleles suggest that the dwarf phenotype is controlled by the same loci in both populations.

Additional Modifiers in the Genetic Background Influence Growth of Incompatible Lines. Even though all of the incompatible lines exhibited dwarfism at low temperature, some variation was observed among them, reflecting incomplete penetrance of the dwarf phenotype in certain lines (*Ler* × Kas-2 RIL 4 in Fig. 2*A*). We concluded that additional modifiers influence growth traits. We developed a near isogenic line (NIL) harboring a *Ler* introgression on QTL 3 in a homogeneous Kas-2 genetic background (Fig. S3). The NIL grown at low temperature exhibited severe stunting that was only partially suppressed by moderate temperature (Fig. 2*A*). Hence, the Kas-2 background in incompatible *Ler* × Kas-2 lines exacerbates growth defects in response to temperature. The flowering time of the NIL was delayed by weeks compared with parental lines when grown on soil at 14 °C (Fig. 2*B*) but resembled the Kas-2 parent when grown at 20 °C (Fig. 2*C*). However, the NIL was ultimately able to flower even under nonpermissive conditions (14 °C) and produce viable seeds. Hence, NIL plants harboring the incompatible allele interaction can still produce progeny and thus overcome complete reproductive isolation. Dwarfism was also suppressed by growing incompatible lines in vitro under high humidity (Fig. 2*D*).

An Interacting Locus on Chromosome 3 Maps to a *RPP1*-Like Cluster. A total of 768 F_2 plants generated from the cross between *Ler* × Kas-2 incompatible lines and Kas-2 and segregating for QTL 3 were used to fine map the locus to a 71.4-kb interval between genes *At3g44600* and *At3g44700* (based on Col sequence; www.arabidopsis.org). In Col, this region contains 11 genes, including 2 *RPP1*-like *TIR-NBS-LRR* genes (13) and 3 transposable elements. A set of 270 F_2 plants derived from a Col and Kas-2

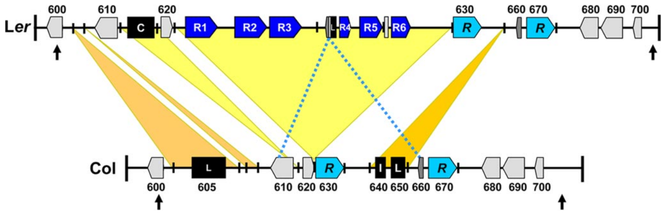

Fig. 3. Comparison of the genetic architecture in QTL 3 between L*er* and Col. Marker positions are indicated by arrows. Insertions are indicated in triangles (yellow in L*er*, orange in Col). Duplications are shown in dotted blue lines. Genes and their orientations are represented. The 3 digits next to the genes are identifiers for the last corresponding AGI numbers (At3g44XXX). The Col At3g44630 and At3g44670 *RPP1*-like genes and homologs in L*er* are shown in light blue. Inserted genes in L*er* encoding TIR-NB-LRR proteins (*R1-R5*) or truncated forms (only TIR domain in *R6*) are indicated in dark blue. Transposable elements are shown in black boxes. C, copia; L, LINE; I, transposase IS4.

cross were grown at low temperature and genotyped. Lines providing Col alleles on QTL 3 and Kas-2 on QTL 4 and 5 did not show stunting, indicating that Col alleles are compatible with Kas-2 and that polymorphism(s) between L*er* and Col lead to incompatibility with Kas-2. The incompatible phenotype was also evident in Landsberg *ERECTA* × Kas-2 F_2 lines (Table S1), thus the L*er* allele on QTL 3 represents a natural allele that was present in the parental Landsberg accession. A BAC spanning QTL 3 in L*er* was isolated from the L*er* BIBAC library (14) and sequenced. Compared with the compatible Col haplotype, the L*er* sequence contains a genomic insertion of 65 kb between At3g44620 and At3g44630 that has 5 genes encoding TIR-NB-LRR proteins (*R1–R5* in Fig. 3) with sequence similarities to *RPP1*-like genes, and 1 gene with a predicted TIR- domain (*R6*; Fig. 3). Together with the *RPP1*-like At3g44630 and At3g44670 homologs in L*er* (630 and 670; Fig. 3) a polymorphic cluster of 7 *TIR-NB-LRR* genes exists in L*er* compared with 2 *TIR-NB-LRR* genes in Col (Fig. 3). The sequences of other genes on QTL 3 At3g44610, At3g44620, At3g44660, At3g44680, At3g44690, and At3g44700 were mostly conserved (Fig. 3). We concluded that one or more L*er* *RPP1*-like gene homologs are the likely determinants of interacting QTL 3. Bomblies *et al.* (7) mapped an interacting QTL for temperature-sensitive hybrid necrosis to the same locus in a cross between Arabidopsis accessions Uk-1 and Uk-3. Hybrids from the cross between L*er* and Kas-2 to Uk-1 and Uk-3 accessions were fully compatible in the F_1 and F_2 generations (Table S1). Thus, the Uk-1 × Uk-3 and L*er* × Kas-2 allele incompatibilities map to an overlapping locus on chromosome 3 but differ in their allelic effects and epistatic interactions (Fig. S2) (7).

Low Temperature Deregulates Cell Death Programs in Incompatible Lines. Temperature and humidity influence the activation of plant defenses against pathogens (11). Dependence of the RIL dwarf phenotypes on these environmental factors and our positioning of QTL 3 to a *RPP1*-like *TIR-NB-LRR* cluster implied that a deregulated TIR-NB-LRR disease-resistance pathway contributes to the L*er* × Kond and L*er* × Kas-2 incompatibilities. We examined dwarf L*er* × Kas-2 RIL and NIL for the occurrence of cell death at low temperature by staining leaves with trypan blue (TB) (15). In all cases, growth at the higher temperature (20 °C) suppressed or attenuated cell death (Fig. 4*A*), consistent with a correlation between cell death and stunting of plant growth. Dispersed areas of necrosis were also seen in the parental Kas-2 line at 14 °C, although L*er* plants did not initiate cell death at either temperature (Fig. 4*A*). Therefore, L*er* and Kas-2 appear to have different thresholds for induction of cell death programs that are revealed at low temperature. Cell

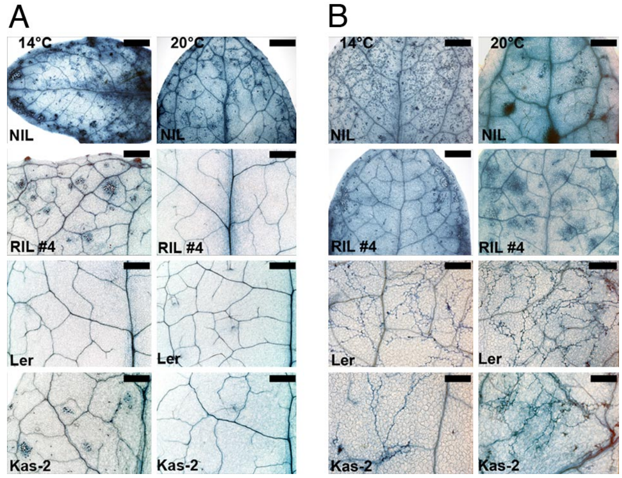

Fig. 4. Cell death and disease-resistance phenotypes of incompatible lines. (*A*) Spontaneous cell death revealed by TB staining of 3-week-old leaves of incompatible lines (4, NIL) and parental accessions grown at 14 °C (*Left*) or 20 °C (*Right*). (*B*) Infection phenotypes of the same lines as in (*A*). Two-week-old plants grown at 14 °C (*Left*) or 20 °C (*Right*) were inoculated with virulent *H. parasitica* isolate Cala2 at 18 °C. Microscopic examination of TB-stained leaves to reveal dead plant cells and pathogen mycelium growth was performed 4 days postinoculation. (Scale bars, 500 μm.)

death also segregated in incompatible L*er* × Kond RILs although neither parent displayed lesions at low temperature (Fig. S4).

QTL governing necrosis at 14 °C were mapped in the L*er* × Kas-2 and L*er* × Kond RIL populations. Four main-effect QTL were identified in L*er* × Kas-2 and L*er* × Kond RILs explaining, respectively, 36% and 42% of the phenotypic variation of cell death (Fig. 1*A*). Three cell-death QTL colocated at the same loci in both populations (Fig. 1*A*) and 2 colocated with previously identified interacting QTL involved in growth variation (QTL 3 and 4; Fig. 1*A*). The average cell death of the different genotypic classes determined by 3-way and 2-way epistatic interactions in L*er* × Kas-2 and L*er* × Kond was measured (Fig. 1*B*) and revealed that combinations of incompatible alleles giving dwarf phenotypes in both populations are also responsible for increased cell death at low temperature (Fig. 1*B*).

Incompatible Lines Exhibit Enhanced Pathogen Resistance. We measured whether the low temperature-conditioned epistatic interactions correlate with increased disease resistance by inoculating L*er* × Kas-2 RIL and NIL with an isolate of the biotrophic oomycete pathogen *Hyaloperonospora parasitica* (Cala2) (16) that infects both parents (Fig. 4*B*). Seedlings were cultivated at 14 °C or 20 °C for 2 weeks and then moved to 18 °C for inoculation, as this is optimal for the pathogen. *H. parasitica* Cala2 was able to colonize L*er* and Kas-2 after growth of plants at low temperature, although pathogen development in Kas-2 was slower than in L*er*, consistent with the occurrence of sporadic cell death in Kas-2 leaves at low temperature (Fig. 4*A* and *B*). Pathogen colonization was strongly inhibited in all incompatible L*er* × Kas-2 lines grown at 14 °C or at 20 °C, as shown for the moderately incompatible RIL 4 and strongly incompatible NIL (Fig. 4*B*). Notably, RIL 4 that exhibited no cell death at 20 °C (Fig. 4*A*) responded to pathogen infection by initiating cell death and resistance in a manner reminiscent of a hypersensitive response (17) (Fig. 4*B*). Lesioning in RIL 4 was dependent on the pathogen because mock-inoculated plants did not initiate cell death (data not shown). We concluded that pathogen infection probably reduces the threshold for activation of defense processes that also lead to hybrid incompatibility at low temperature.

Disproportionate SA Pathway Activation in Incompatible Lines. We selected the L*er* × Kas-2 RIL population for further characterization of plant defense pathway activation. Transcripts of genes regulated by oxidative stress (*GST-1*) (18), SA (*EDS1*, *PR-1*) (19), or jasmonic acid (JA; *PDF1.2*) (19) were quantified by real-time PCR in a set of lines grown at 14 °C and 20 °C. Expression of *GST1*, *EDS1*, and *PR-1* was enhanced in all dwarf lines and in Kas-2 grown at 14 °C compared with 20 °C (Fig. S5). The L*er* parental and semidwarf lines (RILs 4 and 6) exhibited a much less pronounced or no effect of temperature on accumulation of these transcripts. Thus, low temperature-induced expression of *GST1*, *EDS1*, and *PR-1* in dwarf lines broadly correlates with the occurrence of cell death (Fig. 4*A*). Notably, JA pathway activation (as measured by *PDF1.2* expression) was high in Kas-2 but not in the compatible or incompatible lines grown at low temperature (Fig. S5), pointing to a degree of SA and JA pathway deregulation in Kas-2. SA synthesis and/or signaling prevail in the incompatible lines at low temperature because *EDS1* and *PR-1* expression remained high but *PDF1.2* expression was dampened (Fig. S5).

We measured whether the extent of incompatibility in the L*er* × Kas-2 lines correlated with SA accumulation and found that low temperature increased levels of free and total SA in Kas-2 plants and the incompatible lines but not in L*er* or the compatible lines (Fig. S6). Strikingly, the NIL accumulated 2- to 3-fold more free SA than Kas-2 at low and moderate temperature (Fig. S6) and displayed a suppression of JA signaling (as measured by *PDF1.2* expression) that was strongest at low temperature (Fig. S5). The extreme phenotype of the NIL points to the importance of L*er* alleles at QTL 3 for strong activation of the SA pathway in a Kas-2 genetic background.

SA Pathway Activation Is Necessary for Hybrid Incompatibility. We investigated the contribution of SA accumulation to hybrid incompatibility by transforming the moderately incompatible L*er* × Kas-2 RIL 4 with a constitutively expressed bacterial *Salicylate Hydroxylase* gene (*NahG*) that converts SA to catechol (19). Two independent homozygous *NahG* transgenic lines were selected that had detectable *NahG* expression by qRT-PCR (not shown). Incompatible RIL 4 plants have reduced leaf size compared with the parents at low temperature (Fig. 5*A*). In contrast, the rosette area of RIL 4-*NahG* plants was not significantly different to the parental lines (Fig. 5*A*). Both RIL 4-*NahG* lines were susceptible to *H. parasitica* infection at low temperature and did not exhibit cell death in response to the pathogen in contrast to the nontransformed RIL 4 (Fig. 5*B*). Therefore, SA accumulation is necessary for growth retardation and the enhanced resistance response of RIL 4.

RIL 4 and RIL 4-*NahG* were crossed with the extreme dwarf L*er* × Kas-2 NIL. F_1 progeny from each cross differed only in the presence or absence of *NahG* transgene and were homozygous at the incompatible interacting loci (QTL 3, 4, and 5). Growth and resistance phenotypes of the F_1 hybrids were analyzed at low temperature. RIL 4 × NIL F_1 hybrids were dwarf (Fig. 5*A*) and resistant to *H. parasitica* infection (Fig. 5*B*), whereas RIL 4-*NahG* × NIL F_1 hybrids were similar in size to the parental lines (Fig. 5*A*), did not exhibit cell death, and became susceptible to pathogen infection (Fig. 5*B*).

Incompatible phenotypes were also suppressed by depletion of SA through introduction of the *sid2–1* mutant defective in the *isochorismate synthase 2* gene responsible for pathogen-induced SA biosynthesis (20). Quadruple homozygous lines harboring the incompatible allelic interaction on QTL 3, 4, and 5 in a *sid2* genetic background were isolated. These lines were not dwarf at low temperature and did not show spontaneous cell death (Fig. S7 *B* and *D*), whereas a wild-type *SID2* allele conferred stunted growth and spontaneous cell death in the same incompatible genetic background (Fig. S7 *C* and *E*). We concluded that the

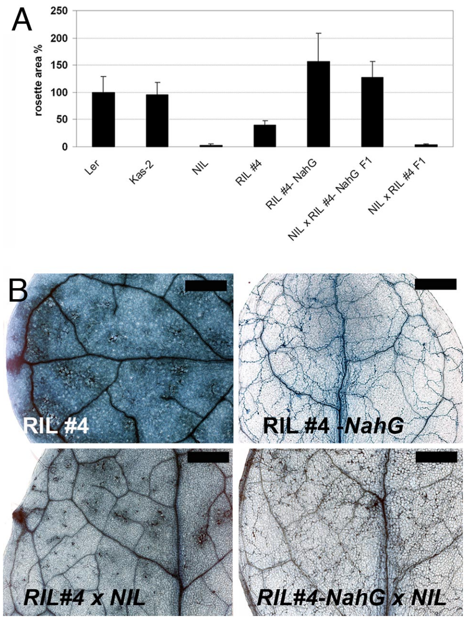

Fig. 5. Suppression of incompatibility by SA depletion. (*A*) Percent rosette area relative to L*er* of 3-week-old plants: incompatible line RIL4 at 14 °C (RIL4), F_1 progeny from a cross between RIL4 and NIL (RIL4 × NIL), RIL4 line transformed with *Salicylate hydroxylase* (RIL4-*NahG*), and F_1 progeny from a cross between RIL4-*NahG* and NIL (RIL4-*NahG* × NIL). (*B*) Infection phenotypes of RIL4, RIL4-*NahG*, RIL4 × NIL, and RIL4-*NahG* × NIL lines (see [*A*] for details of lines). Two-week-old plants grown at 14 °C were inoculated with virulent *H. parasitica* isolate Cala2 at 18 °C. Plant cell death and pathogen colonization was monitored as in Fig. 4. (Scale bars, 500 μm.)

extreme dwarfism, enhanced pathogen resistance, and necrosis exhibited by incompatible lines at low temperature depend on SA accumulation.

We then examined the effect of a mutation in the enhanced disease susceptibility (*EDS1*) gene because this is an essential regulator of SA production and defense signaling triggered by TIR-NBS-LRR resistance proteins (11, 21). A null *eds1* mutant in L*er* (*eds1–2*) was crossed to Kas-2 and 192 F_2 plants genotyped with markers spanning four loci: QTL 3, QTL 4, QTL 5, and *EDS1*. Quadruple homozygous (*eds1–2*/*eds1–2*, QTL 3: L*er*/L*er*, QTL 4: Kas-2/Kas-2, and QTL 5: Kas-2/Kas-2) were isolated. No segregation of dwarfism was observed in progeny from F_2 single-locus segregating lines or *eds1–2* homozygous-incompatible lines grown at 14 °C (Fig. S8). Thus, dwarfism driven by the incompatible allele interaction requires *EDS1.* The *eds1* mutation also restored susceptibility to *H. parasitica* isolate Cala2 in incompatible L*er* × Kas-2 lines grown at low temperature (Fig. S8). These data show that environmentally conditioned activation of immune and cell death responses in the incompatible hybrids requires SA signaling through the EDS1 pathway. They also support our conclusion that a L*er* *TIR-NB-LRR* gene(s) is the determinant of interacting QTL 3.

Discussion

Hybrid vigor, the phenomenon of increased performance of hybrids compared with the parents, is well documented in plant species (22). Reduced viability of hybrids has also been reported and is implicated in the process of speciation (23, 24). In the Dobzhansky-Muller (D-M) model, postzygotic isolation in hybrids arises as a consequence of evolutionary divergence and involves epistatic interactions between different allelic forms (25). Here we describe Arabidopsis epistatic interactions leading to severe growth defects in a specific environment (14 °C). At 20 °C, the defects are fully or partially suppressed (Fig. 2), although a positive trait of enhanced disease resistance is observed (Fig. 4*B*), potentially conferring a selective advantage to these plants when under high pathogen pressure (26, 27). Thus hybrid genotypes with enhanced fitness in one environment may become inferior under different conditions (8). Because D-M incompatibilities accumulate during evolution (25, 28) and we observe residual fertility of hybrids, we propose that additional incompatible loci apart from the 3- or 2-way interacting ones identified (Figs. 1 and S2) may be required for complete hybrid breakdown. Indeed, a contribution of additional loci in L*er* × Kas-2 incompatibilities is suggested by the range of growth and cell death phenotypes observed in incompatible lines sharing common allelic combinations on QTL 3, 4, and 5 (Figs. 2 and 4). Of these lines, L*er* × Kas-2 NIL containing L*er*-derived QTL 3 in a mainly Kas-2 background appears to be at the extreme end of plant stunting and loss of vigor (Fig. 2). An attempt to map these modifiers by simple analysis of cosegregation between the extent of dwarfism at low temperature with the genotype of incompatible lines compared with the NIL was not successful. This suggests that multiple loci with small effects, or other complex epistatic networks not yet identified, act as modifiers of the incompatible phenotypes.

We find that the same interacting QTL conditioned dwarfism and cell death at low temperature (Fig. 1) and conclude that suppression of growth through promotion of cell death underlies the epistatic interactions. Stunting is a common feature of plant mutants that express deregulated defenses and can be associated with spontaneous lesion formation (17). Reduced growth of the plant is thought to be due to the high metabolic cost of maintaining activated resistance pathways (26, 29). Interactions between different hormone systems also influence plant development in response to pathogens (9, 30, 31). In our study, though all dwarf plants exhibited cell death, some normally sized lines were found that also had lesions, consistent with other genes influencing cell death programs that are not linked to growth.

Increased resistance to virulent pathogen (*H. parasitica*) infection coupled with pathogen-induced cell death in leaves of incompatible lines (Fig. 4*B*) is consistent with these plants being primed for resistance through lowering thresholds for the activation of immune responses (Fig. 4*B*) (7, 29). Levels of SA increased dramatically in the incompatible lines at low temperature (Fig. S6). Moreover, the SA pathway was shown to be important for driving hybrid incompatibility as dwarfism and associated cell death in the RIL and NIL were fully suppressed when carrying a dominant *NahG* transgene that depletes SA (Fig. 5), by a mutation of the isochorismate synthase *SID2* gene involved in SA biosynthesis (Fig. S7) or mutations in the SA regulator, *EDS1* (Fig. S8). The degree of SA pathway flux appears to correlate with the extent of hybrid incompatibility (Figs. S5 and S6). It is likely therefore that accumulation of additional D-M incompatibilities and/or the occurrence of more active alleles contributing to SA pathway activation are needed to achieve complete hybrid breakdown seen by Bomblies *et al.* (7). It is notable that SA pathway activation in the RILs and NIL dampened low temperature-induced JA signaling of the Kas-2 parental line (Fig. S5). Kas-2 has hallmarks of a plant genotype that is unable to fine-tune SA-JA pathway crosstalk (19). The introduction of L*er* genes into Kas-2, most obviously the *TIR-NB-LRR* genes residing at QTL 3, causes disproportionate triggering of the SA pathway and a suppression of Kas-2 autoactivated JA signaling.

Autoactivation of immune responses associated with Arabidopsis hybrid breakdown at low temperature has been described (7). This analysis and our findings point to a major influence of temperature and humidity on the degree of epistasis, most likely by altering thresholds for defense and cell death pathway triggering. A number of mutants that have temperature- and/or humidity-sensitive autoimmune responses have been isolated (11). Some of these map to *NB-LRR* genes, supporting the notion that the normal behavior of NB-LRR proteins as constrained sentinels for specific pathogen effectors can be conformationally altered through mutation to give environmentally conditioned constitutive resistance. *NB-LRR* genes on QTL 3 in the incompatible L*er* haplotype are arranged in a cluster of 7 *RPP1*-like genes, instead of the 2 (At3g44630 and At3g44670) present in Col (Fig. 3). Thus, one or more *NB-LRR* genes in L*er* QTL 3 are likely determinants for the incompatibility. Given the large number of polymorphic *R* loci in the Arabidopsis genome (32), the potential for epistatic interactions among them is high. Strikingly, the Uk-1/Uk-3 interacting locus on chromosome 3 described (7) maps to an overlapping region to QTL 3 in the L*er* × Kas-2 RIL population. However, different genetic determinants appear to underlie this epistasis because of the recessive nature of the interacting QTL 3 allele and absence of incompatibilities between L*er* and Kas-2 to Uk-1 and Uk-3 (Table S1) described in our study. Hence, different epistatic networks appear capable of promoting hybrid incompatibilities through environmentally conditioned activation of plant immune responses.

Materials and Methods

Plant Materials and Growth Conditions. Stock numbers for the *Arabidopsis thaliana* accessions are: N20 (L*er*), N1264 (Kas-2), CS6175 (Kond), CS929 (Sha), N8580 (Cvi), N944 (An-1), and CS22548 (Eri-1). Uk-1 (N1575) and Uk-3 (N1577) were provided by K. Bomblies. L*er* × Kas-2 and L*er* × Kond RIL populations were used in this work (12). Plants were germinated and grown in growth chambers (Percival Scientific) under 12 h dark/12 h light cycles at 14 °C/16 °C or 20 °C/22 °C and 70% relative humidity. Three plants per RIL were cultivated, and rosette area was determined in 1-month-old plants. Area measurements were performed with Image Pro Analyzer (Media Cybernetics, Inc.).

QTL Detection and Epistasis. QTL mapping was performed using MapQTL 5.0 software (Kyazma BV) and a common genetic map for L*er* × Kas-2 and L*er* × Kond RIL populations (JoinMap 4; Kyazma BV). A permutation test using 1,000 permutations of the original data resulted in a genome-wide 95% LOD threshold of ≈2.5. The automatic cofactor selection procedure was applied per chromosome to select markers to be used as cofactors for the composite interval mapping (CIM). Markers most closely linked to QTL that appeared only after each round of CIM mapping were also selected as cofactors. The software Epistat (33) has been used to detect pairwise epistatic interactions with a log likelihood ratio (LLR) threshold >6 and at least 8 individuals per subgroup.

Fine Mapping and BAC Sequencing. Fine mapping of QTL 3 was performed in 768 F_2 lines segregating for this locus, and fixed Kas-2 alleles on QTL 4 and QTL 5. These lines were generated from crosses between incompatible L*er* × Kas-2 RILs (nos. 38, 88, and 101) and Kas-2. BAC clones spanning the QTL 3 were isolated from the L*er* BIBAC library (14) by Southern blot hybridization using PCR-amplified flanking markers as probes. BAC sequencing was performed by construction of a shotgun library by Qiagen GmbH. Plasmid clones with 2.5 kb insert size in pUC19 vector were end sequenced on ABI 3730XL system. Base calling was carried out using PHRED (34) and assembly using gap4 from Staden package (35).

Generation of L*er* × Kas-2 NIL. The NIL was obtained by recurrent backcrossing of L*er* × Kas-2 RIL 156 (12) to Kas-2. F_4 NIL plants were genome-wide genotyped with a set of 149 SNP polymorphic between L*er* and Col using Sequenom iPLEX genotyping (Sequenom, Inc.).

Histochemical Analyses. Plant cell death was monitored by staining with lactophenol TB (15). Samples were mounted in 60% glycerol and observed under light microscope (Axioplan; Carl Zeiss) and images captured in a Leica DFC490 digital camera. Extent of cell death was scored by measuring the ratio between the area of stained cells and total leaf area (method detailed in Fig. S9).

Pathogen Infection Assays. The *H. parasitica* Cala2 isolate used in this study has been described previously (15). Two- to 3-week-old plants grown at 14 °C or 20 °C were spray inoculated with a suspension of 4×10^4 conidiospores per milliliter and transferred to optimal conditions for pathogen growth (18 °C).

Plant cell death and *H. parasitica* infection structures were visualized under a light microscope after 4 days of infection by staining of leaves with lactophenol TB (15). Inoculations were performed in at least 6 plants per line, and repeated 3 times with consistent results.

Gene Expression Analyses. Total RNA was isolated from leaves of 3-week-old plants using TRIzol (Invitrogen). One microgram of total RNA was treated with DNase I (Invitrogen) and first-strand cDNA synthesized using SuperScript III (Invitrogen). Quantitative real-time PCR with the SYBR Green I dye method was performed on an Eppendorf Mastercycler detector system. Standard curves were used for quantification. PCR conditions were as follows: 95 °C 2 min, followed by 40 cycles (95 °C, 15 s; 60 °C, 30 s; 68 °C, 20 s). The following gene-specific primers were used: *GST1* (5′TGAACCAACTGGGTCAAACTC and 5′CTTCTCTCAACTGGCAAGGAC), *EDS1* (5′GGAGAATGGATCACAGACGGG and 5′CGTAATCCACCACTTTCTAAACGTT), *PR-1* (5′CTTTGTAGCTCTTGTAGGTGCTCTT and 5′TGGTTGTGAACCCTTAGATAATCTT), and *Actin2* (5′GATTCAGATGCCCAGAAGTCTTGT and 5′TGGATTCCAGCAGCTTCCAT).

Salicylic Acid Quantification. Total and free SA levels were measured in leaves of 3-week-old plants. Leaf material (100–200 mg fresh weight) was extracted with aqueous methanol (36). For total SA measurements, leaf extracts were hydrolyzed with β-glucosidase (EC 3.2.1.21; Sigma-Aldrich), and released SA was re-extracted as described (37). HPLC analyses were performed on an Agilent 1100 HPLC system. Analyses were performed by triplicate in 2 independent experiments with similar results.

Generation of RIL4-*NahG*, RIL6-*sid2–1* and *eds1–2* × Kas-2 Lines. The 35S:*NahG* construct in pBIN19 binary vector (38) was provided by X. Dong. L*er* × Kas-2 RIL 4 plants were transformed (39) and *NahG* expression in transgenic lines was analyzed by qPCR with primers (5′AAGGTATCGCCCAATTCAGGAAG and 5′GCCGTCAAGCCCTAGGTACATCT). To generate L*er* × Kas-2 incompatible lines in *sid2–1* (20) or *eds1–2* (15) genetic backgrounds, *sid2–1* mutant (Col) was crossed to the incompatible L*er* × Kas-2 RIL 6 and *eds1–2* (L*er*) to Kas-2. A total of 192 F_2 plants were genotyped with markers spanning QTL 3, QTL 4, QTL 5, and *SID2* or *EDS1* mutation. Quadruple homozygous lines were isolated at the F_3.

ACKNOWLEDGMENTS. We thank Maarten Koornneef for critical reading of the manuscript and for providing genetic materials. Funding was provided by the Max Planck Society. R.A. acknowledges support from Departament Universitats Recerca i Societat de la Informacío, Generalitat de Catalunya. J.E.P. and A.V.G. acknowledge support of an International Max Planck Research Schools PhD Fellowship to A.V.G.

1. Mitchell-Olds T, Schmitt J (2006) Genetic mechanisms and evolutionary significance of natural variation in Arabidopsis. *Nature* 441:947–952.
2. Abbott RJ, Gomes MF (1989) Population genetic structure and outcrossing rate of *Arabidopsis thaliana* (L.) Heynh. *Heredity* 62:411–418.
3. Tonsor S, Alonso-Blanco C, Koornneef M (2005) Gene function beyond the single trait: Natural variation, gene effects, and evolutionary ecology in *Arabidopsis thaliana. Plant Cell Environ* 28:2–20.
4. Weinreich DM, Watson RA, Chao L (2005) Perspective: Sign epistasis and genetic constraint on evolutionary trajectories. *Evolution* 59:1165–1174.
5. Dobzhansky T (1937) *Genetics and the Origin of Species* (Columbia Univ Press, New York).
6. Muller H (1942) Isolating mechanisms, evolution, and temperature. *Biol Symp* 6:71–124.
7. Bomblies K, *et al.* (2007) Autoimmune response as a mechanism for a Dobzhansky-Muller-type incompatibility syndrome in plants. *PLoS Biol* 5:e236.
8. Bordenstein S, Drapeau M (2001) Genotype-by-environment interaction and the Dobzhansky & Muller model of postzygotic isolation. *J Evol Biol* 14:490–501.
9. Robert-Seilaniantz A, Navarro L, Bari R, Jones JD (2007) Pathological hormone imbalances. *Curr Opin Plant Biol* 10:372–379.
10. Botella MA, *et al.* (1998) Three genes of the Arabidopsis RPP1 complex resistance locus recognize distinct *Peronospora parasitica* avirulence determinants. *Plant Cell* 10:1847–1860.
11. Wiermer M, Feys BJ, Parker JE (2005) Plant immunity: The EDS1 regulatory node. *Curr Opin Plant Biol* 8:383–389.
12. El-Lithy ME, *et al.* (2006) New Arabidopsis recombinant inbred line populations genotyped using SNPWave and their use for mapping flowering-time quantitative trait loci. *Genetics* 172:1867–1876.
13. Meyers BC, Kozik A, Griego A, Kuang H, Michelmore RW (2003) Genome-wide analysis of NBS-LRR-encoding genes in Arabidopsis. *Plant Cell* 15:809–834.
14. Chang YL, Henriquez X, Preuss D, Copenhaver G, Zhang H-B (2003) A plant-transformation-competent BIBAC library from the *Arabidopsis thaliana* Landsberg ecotype for functional and comparative genomics. *Theor Appl Genet* 106:269–276.
15. Feys BJ, *et al.* (2005) Arabidopsis senescence-associated gene101 stabilizes and signals within an enhanced disease susceptibility1 complex in plant innate immunity. *Plant Cell* 17:2601–2613.
16. Holub EB, Beynon JL (1997) in *Advances in Botanical Research: Incorporating Advances in Plant Pathology*, eds Andrews JH, Tommerup IC (Academic, San Diego), pp 227–273.
17. Jones JDG, Dangl JL (2006) The plant immune system. *Nature* 444:323–329.
18. Rentel MC, Knight MR (2004) Oxidative stress-induced calcium signaling in Arabidopsis. *Plant Physiol* 135:1471–1479.
19. Glazebrook J (2005) Contrasting mechanisms of defense against biotrophic and necrotrophic pathogens. *Annu Rev Phytopathol* 43:205–227.
20. Wildermuth MC, Dewdney J, Wu G, Ausubel FM (2001) Isochorismate synthase is required to synthesize salicylic acid for plant defence. *Nature* 414:562–565.
21. Wirthmueller L, Zhang Y, Jones JDG, Parker JE (2007) Nuclear accumulation of the Arabidopsis immune receptor RPS4 is necessary for triggering EDS1-dependent defense. *Curr Biol* 17:2023–2029.
22. Shull G (1922) About the heterozygosity regarding the success in practical breeding (German). *Beitr Pflanzenzucht* 5:134–158.
23. Coyne J, Orr H (2004) *Speciation* (Sinauer Associates, Sunderland, MA).
24. Bomblies K, Weigel D (2007) Hybrid necrosis: Autoimmunity as a potential gene-flow barrier in plant species. *Nat Rev Genet* 8:382–393.
25. Orr HA, Turelli M (2001) The evolution of postzygotic isolation: Accumulating Dobzhansky-Muller incompatibilities. *Evolution* 55:1085–1094.
26. Tian D, Traw MB, Chen JQ, Kreitman M, Bergelson J (2003) Fitness costs of R-gene-mediated resistance in *Arabidopsis thaliana. Nature* 423:74–77.
27. Traw MB, Kniskern JM, Bergelson J (2007) SAR increases fitness of *Arabidopsis thaliana* in the presence of natural bacterial pathogens. *Evolution* 61:2444–2449.
28. Welch JJ (2004) Accumulating Dobzhansky-Muller incompatibilities: Reconciling theory and data. *Evolution* 58:1145–1156.
29. van Hulten M, Pelser M, van Loon LC, Pieterse MJP, Ton J (2006) Costs and benefits of priming for defense in Arabidopsis. *Proc Natl Acad Sci USA* 103:5602–5607.
30. Wang D, Pajerowska-Mukhtar K, Culler AH, Dong X (2007) Salicylic acid inhibits pathogen growth in plants through repression of the auxin signaling pathway. *Curr Biol* 17:1784–1790.
31. Navarro L, *et al.* (2008) DELLAs control plant immune responses by modulating the balance and salicylic acid signaling. *Curr Biol* 18:650–655.
32. Clark RM, *et al.* (2007) Common sequence polymorphisms shaping genetic diversity in *Arabidopsis thaliana. Science* 317:338–342.
33. Chase K, Adler F, Lark K (1997) Epistat: A computer program for identifying and testing interactions between pairs of quantitative trait loci. *Theor Appl Genet* 94:724–730.
34. Ewing B, Hillier L, Wendl MC, Green P (1998) Base-calling of automated sequencer traces using Phred. I. Accuracy assessment. *Genome Res* 8:175–185.
35. Bonfield JK, Smith KF, Staden R (1995) A new DNA sequence assembly program. *Nucl Acids Res* 23:4992–4999.
36. Bednarek P, Schneider B, Svatos A, Oldham NJ, Hahlbrock K (2005) Structural complexity, differential response to infection, and tissue specificity of indolic and phenylpropanoid secondary metabolism in Arabidopsis roots. *Plant Physiol* 138:1058–1070.
37. Lee H-i, Raskin I (1998) Glucosylation of salicylic acid in *Nicotiana tabacum* cv. Xanthi-nc. *Phytopathology* 88:692–697.
38. Bowling SA, *et al.* (1994) A mutation in Arabidopsis that leads to constitutive expression of systemic acquired resistance. *Plant Cell* 6:1845–1857.
39. Bechtold N, Pelletier G (1998) in *Arabidopsis Protocols*, eds Martinez-Zapater JM, Salinas J (Humana, Totowa, NJ), pp 259–266.

PLANT BIOLOGY